Wide angle mirror system design for distortionless imaging of the sky

Michael J. Kosch,[1,*] Todd Pedersen,[2] and Robert Esposito[2]

[1]Communication Systems, Lancaster University, Lancaster LA1 4WA, UK

[2]Space Vehicles Directorate, Air Force Research Laboratory, Hanscom Air Force Base, Massachusetts 01731, USA

*Corresponding author: m.kosch@lancaster.ac.uk

Received 22 May 2009; revised 30 July 2009; accepted 30 July 2009; posted 31 July 2009 (Doc. ID 111773); published 0 MONTH 0000

We describe a dual-mirror wide angle optical design, which removes the radial distortion associated with traditional all-sky optics for a chosen altitude. The wide angle mirror system provides a transform of the sky, for a selected altitude, as if the viewer is situated at the center of the Earth. Other advantages of the system include (1) real time achromatic transform, (2) higher optical gain compared to pure lens systems, (3) a quasi-telecentric optic capable of taking narrowband interference filters without modification, and (4) a uniform sky spatial resolution everywhere on the detector. Disadvantages include (1) cost of manufacture and (2) focusing issues, especially near the horizon. © 2009 Optical Society of America

OCIS codes: 230.4040, 110.2970, 010.0280.

1. Introduction

Imaging the nighttime sky using all-sky lenses of 180° field of view, called all-sky imaging, has a long tradition in atmospheric airglow and auroral science dating back more than 50 years to before the International Geophysical Year in 1957 (cf. [1,2]). Fundamentally, a single or dual mirror system with focusing lens, or a pure lens, is used to form a round image. If the camera is mounted pointing vertically, then the image is circularly linear in azimuth angle about the camera and radially linear from the image center in zenith angle with the local horizon appearing around the edge of the circular image [1]. For an altitude of 100 km, where the maximum brightness in auroral emissions typically occurs [2], an all-sky imager gives a radial field of view of ~500 km.

The circular all-sky images are generally processed into either geographic coordinates [3] or a regular spatial grid of constant size [4], for a chosen altitude. Unfortunately, this significantly reduces the image spatial resolution of same sized features in the sky away from the local zenith. This is illustrated in Fig. 1, which shows a regular grid of 0.1° latitude and 0.25° longitude at 100 km altitude, corresponding to approximately 10 × 10 km squares to within 10%, covering 5° in latitude and 12.5° in longitude, for a high latitude site [5]. For CCD technology with its regular rectangular array of pixels, the number of pixels contributing to each trapezoid and therefore the optical signal-to-noise ratio decreases with increasing zenith angle. One objective of the design described below is to eliminate this effect. Radic and Andreic [6] and Andreic and Radic [7] effectively did this with their all-sky single mirror design, which gave constant angular magnification. However, they did not address the problem of fixed altitude in the sky nor the fact that the camera blocks the local zenith. We solve both these problems together.

2. Design

Figure 2 illustrates the transform required to eliminate the all-sky circular distortion and produce a

0003-6935/09/260001-01$15.00/0

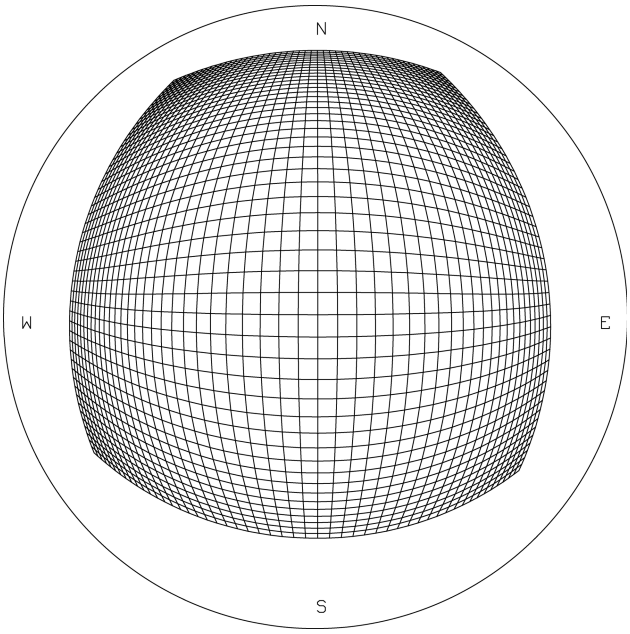

Fig. 1. Geographic grid covering 67.6°–72.6° N, 13.5°–26.0° E, in steps of 0.1° latitude and 0.25° longitude, at an assumed altitude of 100 km as seen through an all-sky lens from 69.35° N, 20.36° E in geographic coordinates. The data grid corresponds to approximately 10 × 10 km trapezoids.

constant sky spatial resolution within the image for a chosen altitude for a vertically pointing camera [8]. The view must be mapped from the local zenith angle (θ) to the angle subtended at the center of the Earth (ε). For a vertically pointing camera, the image will remain azimuthally symmetric about the line connecting the camera to the center of the Earth. For the Earth radius (r) and a user selected altitude (h), it is easily shown that [8]

$$\tan(\theta) = \frac{(h+r)\sin(\varepsilon)}{(h+r)\cos(\varepsilon) - r}. \quad (1)$$

To achieve full all-sky imaging ($\theta = \pm 90°$), $\varepsilon \approx \pm 10°$. However, by limiting θ to $\pm 75°$, which is often sufficient for real applications, $\varepsilon \approx \pm 3°$. This offers significant advantages in terms of mirror manufacturing effort, the use of interference filters and focusing, as discussed below.

Figure 3(a) is a schematic of a traditional all-sky single mirror system (top) and the image produced on a square detector (bottom). Typically, the curvature of the mirror is constant such that the image is radially linear in local zenith angle for a vertical pointing imager. An obvious problem is that the camera blocks the local zenith (black disk), which is often the most interesting part of the sky for a particular imager placement. The constant angular magnification all-sky mirror design by Radic and Andreic [6] and Andreic and Radic [7] also suffers from this problem. In some designs, a secondary mirror is used, allowing the camera to be located somewhere more convenient, but this does not solve the problem of

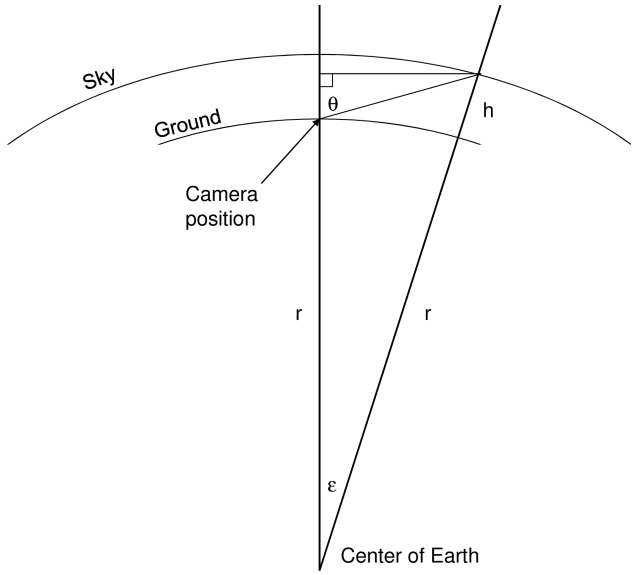

Fig. 2. Geometry showing the transform implemented, where r is the radius of the Earth, h is the transform altitude, θ is the local zenith angle, and ε is the angle subtended at the center of the Earth.

zenith blocking. In order to substitute ε for θ in Fig. 3(a), the curvature of the mirror is adjusted as a function of radius for the desired transform altitude using Snell's law of reflection. Hough and Scourfield [9] produced the wide angle no distortion (WAND) all-sky mirror system, which implemented Eq. (1). However, the problem of zenith blocking remained. Here we solve this problem.

A solution to zenith blocking is shown schematically in Fig. 3(b). The mirror curvature is such that its highest point is not in the center, as is the case in Fig. 3(a), but forms a doughnut. The negative slope of the mirror surface near the central axis allows rays from the local zenith to reach the mirror and be reflected into the focusing lens. The hole in the middle of the mirror is not relevant to the optics but can be used to accommodate the camera if a secondary mirror is implemented. The curvature of the mirror can be arranged such that the image is linear in θ or ε. Either way, the local zenith forms a circle about the center of the detector (black disk), which contains no useful information. This cosmetic blemish can be removed by a suitable secondary mirror, as described below. The fact that the vertical rays come from a cylinder of finite diameter is of no practical consequence because the cylinder diameter is small compared to the projection altitude of 100 km.

If a transform is implemented with a dual mirror design, great flexibility is afforded and many nonunique solutions are possible. Three basic classes of dual mirror design are possible, with the primary–secondary being convex–convex, concave–concave, and convex–conical. Andreic and Radic [10] produced a near all-sky imager using a single concave mirror. They found that a full 180° field of view could not be achieved, but failed to realize the problem could be solved by a secondary concave mirror. However, they

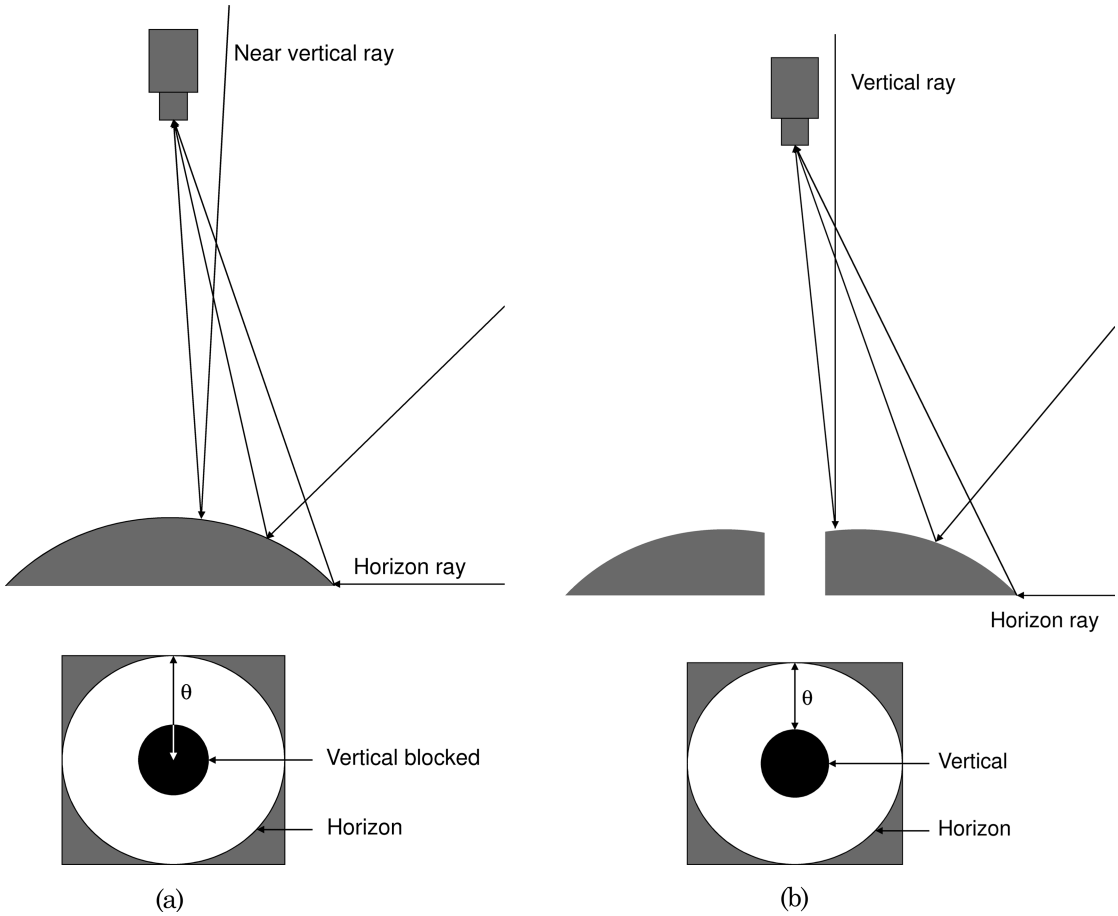

Fig. 3. (a) Schematic of a traditional all-sky mirror lens (top) and the resulting image (bottom). The black disk represents the image area that is blocked by either the detector or a secondary mirror. The image radius linear in θ (or ε) is shown. (b) Schematic of a modified traditional all-sky mirror lens (top) and the resulting image (bottom). The maximum height of the primary mirror is not in the center but forms a doughnut. The black disk contains no useful information in the image. The image radius linear in θ (or ε) is shown.

did show that the convex mirror design produces a more compact system, for the same focus performance, than the concave mirror design. This is because the convex mirror produces its virtual image behind the mirror surface, whereas the concave mirror has its virtual image in front of the mirror surface. To achieve the same focus performance, the convex mirror requires the camera–mirror distance to be less than a similar concave mirror. All combinations of convex and concave mirrors were investigated, but the convex–conical design is easiest to manufacture because one mirror has a pure conical surface and provides the best overall focus by maximizing the camera to virtual image distance, as discussed below.

Table 1. Parameters Associated with the WAMS Design Shown in Fig. 4 for a Transform Altitude of 100 km[a]

Dimension	Size (in.) or Angle (deg.)
ε and θ	10.0° and 89.9°
Secondary cone angle	5.0°
Secondary radius = primary hole	3.17 in.
Secondary apex distance from origin	18.0 in.
Primary x-axis radius	11.78 in.
Primary max/min y-axis dimension	+0.00453/ − 5.23 in.
Closest focus y-position/total distance	−0.56/36.84 in.

[a]The focusing lens is placed at the system origin.

Figure 4(a) shows a schematic of the dual mirror wide angle mirror system (WAMS) for $\theta \approx \pm 90°$. The focusing lens is placed at the system origin. From an optical point of view, the only fundamental difference between Figs. 3(b) and 4(a) is the cone-shaped secondary mirror. However, the secondary mirror allows for the incoming vertical rays to be reflected via both mirrors into the center of the lens. Hence, in this design, the primary mirror performs the transform described by Eq. (1), while the secondary removes the cosmetic blemish shown in Fig. 3(b). Due to manufacturing limitations, the central image pixel, which views the apex of the secondary mirror cone, may not contain any useful information. Figure 4(a) shows that an image radially linear in ε will be produced where the local zenith is in the middle of the image.

Table 1 gives the important dimensions in inches (1 in. =2.54 cm) for the WAMS shown in Fig. 4(a). Reflective optics scale linearly, so the transform is unaffected by physical size. The dimensions given allow the device to be mounted in a standard 40

in. (1.016 m) acrylic hemispherical dome. There are only three free parameters, which the user can manipulate. First, there is the transform altitude, which is set to 100 km in Fig. 4(a). As the transform altitude approaches infinity, or at least ten Earth radii, the primary mirror automatically assumes the shape of a traditional all-sky optic, i.e., constant curvature. Second is the origin-to-secondary mirror apex distance, which determines the overall scaling, and is set to 18 inches in Fig. 4(a) according to practical housing limitations. Third is maximum value of ε, which determines the field of view (2θ) from Eq. (1) and the maximum diameter of both mirrors. In Fig. 4(a), $\varepsilon = 10°$, giving $\theta = 89.9°$ and total field of view of 179.8°. Alternately, $\varepsilon = 3°$, which gives $\theta = 74.9°$ and total field of view of 149.8°. The cone angle of the secondary mirror is automatically set to ensure that the vertical rays will appear in the center of the image. The secondary is near flat with the cone angle of 5° (see Table 1). The numerical integration to determine the shape of the primary proceeds toward increasing diameter (from vertical to horizon rays) from the y-axis origin with the x-axis starting point determined by the secondary mirror size [3.17 inches in Fig. 4(a)]. The radius of the secondary mirror is automatically set from the user selection of the free parameters.

A few other issues are worth addressing. First, the focal length of the focusing lens has no bearing on the transform described in Eq. (1), provided the angular field of view of the lens is linear with image radius from the center of the image. Changing the focal length merely changes the image size on the detector. The lens field of view (FOV) is given by

$$\mathrm{FOV} = 2\tan^{-1}\left(\frac{d}{2f}\right), \tag{2}$$

where d is the detector size and f is the lens focal length [11] and $\mathrm{FOV} = 2\varepsilon$ for WAMS. For a typical auroral imager CCD with 512×512 pixels of $25\,\mu$m size square, $d = 12.8$ mm (nominally ½ inch), giving $f = 36.3$ mm for $\varepsilon = 10°$ or $f = 122.1$ mm for $\varepsilon = 3°$. Second, the aperture of typical focusing lenses can be F1 or better, for moderate cost, whereas the commercial all-sky lenses are typically F4 or F2.8 at best. The light gathering power of an F1 lens is 16× greater than that of F4, a significant advantage for nighttime all-sky imaging. Third, since the mirrors are achromatic light reflectors, the transform is scale invariant. Hence the use of arbitrary units in Fig. 4(a). The size of the mirrors is determined by other considerations, e.g., manufacturing costs and housing limitations. However, WAMS should be made as large as reasonably possible for focusing reasons, as discussed below. Fourth, a wavelength selective interference filter can be inserted at any point between the secondary mirror and focusing lens. Interference filters change the wavelength of their passband according to the angle of incidence as follows:

$$\frac{\lambda_\varepsilon}{\lambda_0} = \sqrt{1 - \left(\frac{N_m}{N_f}\right)^2 \sin^2(\varepsilon)}, \tag{3}$$

where λ_ε is the wavelength at the angle of incidence (ε), λ_0 is the wavelength at normal incidence, N_m is the refractive index of the medium (1 for air), and N_f is the refractive index of the interference filter (typically ≅2). For a typical visible auroral wavelength of 557.7 nm, the shift in filter wavelength is 2.1 nm for $\varepsilon \le 10°$, which gives the minimum filter bandwidth to view the line emission. This increases to 3.2 nm for an infrared auroral emission at 844.6 nm. Since it is uncommon that a narrower bandwidth is required for auroral applications, WAMS requires no addi-

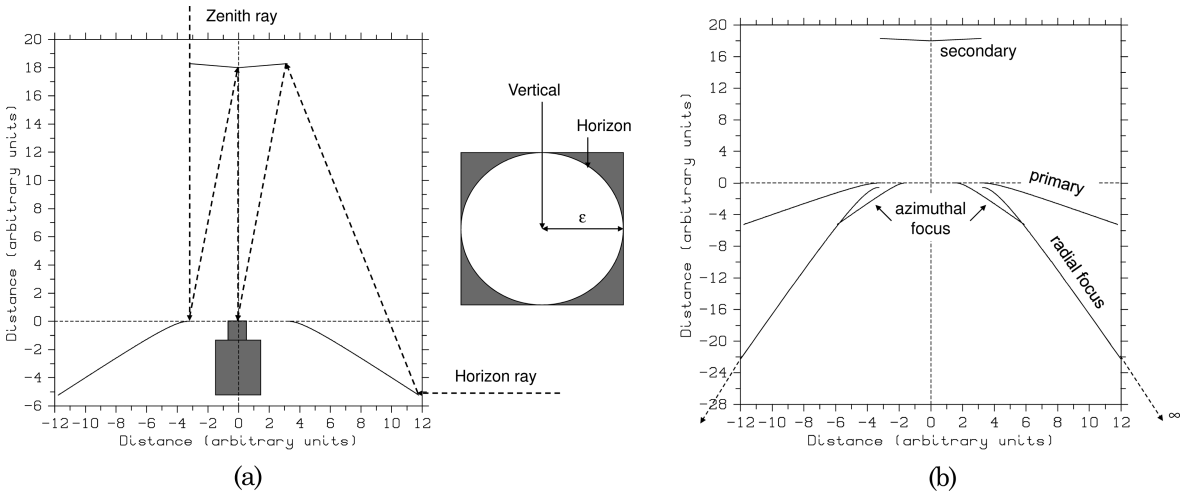

Fig. 4. (a) Schematic of the wide angle mirror system as implemented (left) and the resulting image (right). The primary mirror (bottom) performs the transform. The secondary mirror ensures that the local zenith is in the middle of the image with no cosmetic artifacts. The image radius linear in ε (or θ) is shown. The scale is arbitrary, but inches give realistic dimensions. (b) Schematic of the wide angle mirror system as implemented, showing the primary and secondary mirrors as well as the locus of radial and azimuthal focus of the primary mirror for objects at infinity. The scale is arbitrary, but inches give realistic dimensions.

tional optics or modifications for its intended application. If $\varepsilon \le 3°$ is used, then the minimum filter bandwidth reduces to 0.2 and 0.3 nm for 557.7 and 844.6 nm, respectively.

Finally, fifth, a potentially serious limitation of WAMS is the issues of focus and astigmatism. Following the procedure by Radic and Andreic [6], Fig. 4(b) shows the WAMS surfaces as well as part of the locus of apparent radial focus for objects at infinity. Where the primary mirror has its maximum curvature (near zenith rays) the image appears to come from close behind the mirror surface [6] (~ -0.56 in. below the origin), i.e., a total distance of ~36.8 in. from the focusing lens. Where the primary mirror has almost zero curvature (near horizon rays) the image appears to come from effectively infinity (not shown). The secondary mirror does not affect the apparent focus in the radial direction because it is perfectly flat in this direction. Hence the focusing lens has to accommodate all object distances from ~36.8 in. to infinity. For geophysical applications, the horizon is usually the least interesting part of the sky. If the field of view is limited to $\theta = \pm 75°$, then the image appears to come from ~ -8.0 in. behind the mirror surface for the maximum zenith angle, which is an object distance of ~45.5 in. from the focusing lens. This significantly reduces the focal range to 36.8–45.5 in. In addition, restricting the field of view produces a more compact design [10], as both primary and secondary mirrors have significantly reduced diameters, i.e., less than a third of full size in this case.

In the azimuthal direction, both the primary and secondary mirrors have curvature, which varies with radius. This should introduce variable astigmatic focus as a function of radius. Unfortunately, astigmatism should be worse for WAMS compared to constant curvature all-sky mirrors [7]. For spherical mirrors, the focal point for objects at infinity is half the radius of curvature. From Table 1, the primary mirror azimuthal focus varies from 1.59 in. for vertical rays to 5.89 in. for horizon rays. Figure 4(b) shows the locus of apparent azimuthal focus of the primary mirror for objects at infinity. It is obvious that the focusing lens needs to accommodate a much smaller range of azimuthal focus than the radial focus described above. Given that the primary mirror is close to the secondary mirror, and that the secondary mirror has a smaller radius of curvature than the primary mirror, the range of azimuthal focus in the final image is compressed even further. Hence the quality of focus is primarily determined by the radial direction. In addition, Radic and Andreic [6] point out that astigmatism is likely not a serious problem, as each point on the convex primary mirror is associated with a different part of the sky. The bundle of rays that makes up each point in the image is infinitesimally small, and astigmatism cannot occur for a single ray. This is borne out by practical experience.

The focusing lens has to accommodate apparent objects over a range of distances using its depth of field, expressed as

$$D_n = \frac{cFs(s-f)}{f^2 + cF(s-f)}, \tag{4a}$$

$$D_f = \frac{cFs(s-f)}{f^2 - cF(s-f)}, \tag{4b}$$

where D_n and D_f are the near and far distances from best focus, respectively, s is the lens focus distance, f is the lens focal length, c is the circle of confusion size, and F is the lens F-number given by $F = f/a$, where a is the lens aperture [11]. The depth of field decreases as the focus is reduced from infinity, the focal length or lens aperture is increased, or the circle of confusion size is decreased. For WAMS, the image focal distance is short (≥ 36.8 in.) and a wide aperture is highly desirable for night vision applications, both of which reduce the depth of field. The depth of field can be increased by reducing the focal length of the focusing lens but this also reduces the image size on the detector by increasing the circle of confusion size, but this also reduces the image resolution, or by increasing the lens F-number [7] but this also reduces the light throughput. The only free parameter is the focus distance, which should be maximized by scaling up the mirror size as far as possible [7]. If the focus is set to 40.4 in. for $\theta = \pm 75°$, then the near and far depths of field are both 0.061 in., which is obviously insufficient to cover the image focal range of 36.8–45.5 in. To accommodate the entire depth of field, either the F-number must be increased to $F = 58.8$, with ~4000× light intensity loss compared to $F = 1$, or the circle of confusion must increase to ~1.5 mm, with loss of image resolution. Ultimately, the user must compromise and choose which part of the field of view to optimize the focus on.

In terms of focus, the primary–secondary convex–conical design presented is one of the best options because the camera to virtual image distance is maximized, a major reason for choosing this design. However, for the concave–concave design, a much narrower depth of field requirement may be possible because the concave mirrors compress the virtual image in front of the mirror surface. This remains to be investigated.

3. Conclusion

A wide angle mirror system (WAMS) has been designed for distortion-free and blemish-free wide field of view imaging of the sky for a selected altitude. If the user is willing to accept the cost of manufacture and modest loss of focus, especially for large viewing angles, then the WAMS offers significant advantages over traditional all-sky lenses. These include (1) distortion-free achromatic imaging for a selected altitude, (2) uniform sky spatial resolution everywhere on the detector, (3) a high light gathering capability more than an order of magnitude greater than commercially available all-sky lenses, and (4)

narrowband interference filters that can be inserted without modification or additional optics.

This work was supported by the U.S. Air Force Office of Scientific Research (AFOSR) task 2311AS. M. J. Koesch acknowledges support by the National Research Council Research Associateship program.

References

1. C. Lance and R. H. Eather, "HAARP Imager," Report ADA- 277469 (Defense Technical Information Center, 1993).
2. C. Stormer, *The Polar Aurora* (Oxford University, 1955).
3. M. J. Kosch, M. W. J. Scourfield, and E. Nielsen, "A self-consistent explanation for a plasma flow vortex associated with the brightening of an auroral arc," J. Geophys. Res. **103**, 29383–29391 (1998).
4. F. J. Garcia, M. J. Taylor, and M. C. Kelley, "Two-dimensional spectral analysis of mesospheric airglow image data," Appl. Opt. **36**, 7374–7385 (1997).
5. M. J. Kosch, T. Hagfors, and E. Nielsen, "A new Digital All-Sky Imager experiment for optical auroral studies in conjunction with the STARE coherent radar system," Rev. Sci. Instrum. **69**, 578–584 (1998).
6. N. Radic and Z. Andreic, "Aspheric mirror with constant angular magnification," Appl. Opt. **31**, 5915–5917 (1992).
7. Z. Andreic and N. Radic, "Aspheric mirror with constant angular magnification II," Appl. Opt. **33**, 4179–4183 (1994).
8. G. Hough, "Evolution of periodicity and scale length in auroral dynamics," Ph.D. thesis (University of Natal, 1994).
9. G. Hough and M. W. J. Scourfield, "WAND auroral imager for SANAE," S. Afr. J. Antarct. Res. **21**, 113 (1991).
10. Z. Andreic and N. Radic, "All-sky camera with a concave mirror," Appl. Opt. **35**, 149–153 (1996).
11. A. R. Greenleaf, *Photographic Optics* (MacMillan, 1950).

Queries

1. This query was generated by an automatic reference checking system. References [4, 5, 6, 7, 9, 10] could not be located in the databases used by the system. While the references may be correct, we ask that you check them so we can provide as many links to the referenced articles as possible.
2. A check of online databases revealed a possible error in Ref. [3]. The date has been changed from '1998a' to '1998'. Please confirm this is correct.
3. Please give page range.